

## CAESIUM IONS ACTIVATE CHLORIDE CHANNELS IN RAT CULTURED SPINAL CORD NEURONES

BY D. HUGHES, R. N. MCBURNEY, S. M. SMITH AND R. ZOREC\*

*From the MRC Neuroendocrinology Unit, Newcastle General Hospital,  
Westgate Road, Newcastle upon Tyne NE4 6BE*

(Received 24 October 1986)

### SUMMARY

1. Caesium ions ( $\text{Cs}^+$ ), applied extracellularly, caused a decrease in the input resistance of cultured spinal cord (s.c.) neurones and depolarized the neurones when they contained 140 mM- $\text{CsCl}$ .

2. The reversal potential for  $\text{Cs}^+$ -activated currents shifted 56 mV on average for a 10-fold reduction in the intracellular chloride ion ( $\text{Cl}^-$ ) activity, indicating that the  $\text{Cs}^+$ -activated currents were specific to  $\text{Cl}^-$ .

3. The activation of  $\text{Cl}^-$  currents by  $\text{Cs}^+$  was not due to the depolarization-evoked release of neurotransmitter from presynaptic terminals. We therefore suggest that  $\text{Cs}^+$  were acting directly on the extracellular surface of the s.c. neurones to activate  $\text{Cl}^-$  currents.

4.  $\text{Cs}^+$ -activated currents showed desensitization in the presence of 140 mM- $\text{Cs}^+$ .

5. The log-log plot of the dose-response data could be fitted with a straight line with a slope of  $1.7 \pm 0.4$  ( $n = 6$ ), indicating that at least 2  $\text{Cs}^+$  were needed to activate a single  $\text{Cl}^-$  channel. The  $K_D$  of the  $\text{Cs}^+$ -induced response was greater than 69 mM.

6. In outside-out patches  $\text{Cs}^+$  activated single  $\text{Cl}^-$  channels. These channels were not activated by sodium or potassium ions.

7. The  $\text{Cs}^+$ -activated channels displayed a total of five distinct conductance states which had mean conductances of 20, 30, 43, 66 and 92 pS. The 30 and 43 pS states were the most frequently occurring states.

8. The conductance states of the  $\text{Cs}^+$ -activated channel have the same conductances as those reported for  $\gamma$ -aminobutyric acid (GABA)- and glycine-activated channels in rat s.c. neurones. We therefore conclude that  $\text{Cs}^+$  activate the same type of  $\text{Cl}^-$  channel as GABA and glycine through an unidentified receptor.

### INTRODUCTION

Recently, during an investigation of the  $\gamma$ -aminobutyric acid (GABA)- and glycine-activated chloride ion ( $\text{Cl}^-$ ) channels in spinal cord (s.c.) neurones, we replaced the monovalent cations in the cells' bathing medium with caesium ions ( $\text{Cs}^+$ ). As  $\text{Cs}^+$

\* Present address: Institute of Pathophysiology, Medical Faculty, P.O. Box 11, 61105 Ljubljana, Yugoslavia.

block certain potassium ion ( $K^+$ ) channels and do not pass easily through sodium ion ( $Na^+$ ) channels (Hille, 1984) we had believed that this exchange of ions would prevent the contamination of our experimental records by cation-conducting channels, and so enable us to study transmitter-activated  $Cl^-$  channels in isolation. Curiously, we found that the application of  $Cs^+$  to the extracellular surface of these cells caused an increase in their membrane permeability to  $Cl^-$ . We therefore decided to investigate this action of  $Cs^+$  on s.c. neurones, both because the observation itself seemed rather surprising and because of the suggested physiological importance of a  $Cl^-$  channel activated by alkali metal ions (Geletyuk & Kazachenko, 1985).

In this paper we report that  $Cs^+$  directly activate  $Cl^-$  channels in s.c. neurones in a dose-dependent manner and that the channels have the same conductance properties as GABA- and glycine-activated channels. A preliminary report of this work has been communicated to the Physiological Society (McBurney, Smith & Zorec, 1985*b*).

#### METHODS

##### *Tissue culture*

A pregnant rat was decapitated 13–15 days after mating and its embryos removed. Spinal cords were dissected from the embryos and placed in an ice-cooled phosphate-buffered saline. The cords were minced with two scalpels and then mechanically dissociated by being passed through syringe needles of decreasing diameter 10–15 times. Needles of 19, 21 and occasionally 23 gauge were used to produce a cloudy cell suspension. The dissociated spinal cords were then plated on to a bed of near confluent cerebral cortex astrocytes at a density of 5000–60000 cells per well. The astrocytes were supported by a collagen-coated, 1 cm square plastic cover-slip (Aclar, Allied Corporation) which was covered by 0.5 ml medium. In this form the cells were incubated at 35 °C in an atmosphere of 5%  $CO_2$  and 95% air. The medium used for the s.c. neurones was either Dulbecco's minimum essential medium (MEM) or a mixture of Dulbecco's MEM, Hams F12 and  $\alpha$ -MEM in the ratio of 3:6:1 (all media obtained from GIBCO). The medium was changed twice weekly. Rat serum, chick embryo extract (GIBCO) and L-glutamine (200 mM, GIBCO) were added to both types of media to produce final concentrations of 4, 1 and 1% (v/v) respectively. Cell-covered cover-slips were selected for experimentation after 8–37 days in culture.

##### *Recording techniques*

Recording pipettes were prepared with outer diameters of about 1–2  $\mu m$  (3–15  $M\Omega$ ) and heat polished according to the methods of Corey & Stevens (1983).

All recordings were made using the whole-cell recording, inside-out or outside-out membrane configurations (Hamill, Marty, Neher, Sakmann & Sigworth, 1981) from s.c. neurones of 10–25  $\mu m$  in diameter. The cells were viewed at  $\times 400$  magnification with an inverted phase-contrast microscope (Zeiss). Experiments were performed using an EPC-5 or EPC-7 amplifier (List Electronics), both of which were modified to permit the offsetting of junction potentials of up to  $\pm 100$  mV. Current and voltage signals were low-pass filtered (1 or 3 kHz) and then recorded on a FM tape-recorder (Racal 4DS) at a bandwidth of d.c. to 2.5 kHz ( $-3$  dB) for later analysis. Records were analysed by replaying the tape-recording and capturing events on the screen of a digital oscilloscope. Measurements were made either directly from the oscilloscope screen or from traces subsequently plotted on a chart-recorder.

##### *Solutions*

During experiments the cover-slips were placed in a chamber (see Fig. 1 of McBurney & Neering, 1985) and continuously superfused with bathing medium. The composition of bathing media and electrode-filling solutions used are described in Table 1. In some experiments tetrodotoxin (TTX) and cadmium ions ( $Cd^{2+}$ ) were added to the bath and test solutions. Such modifications to any solutions are described in the relevant Figure legends.

Test solutions were applied to whole cells and outside-out patches by pressure ejection ( $< 0.05 \text{ N m}^{-2}$ ) from large-diameter micropipettes (2–10  $\mu\text{m}$  outer tip diameter), by bath application or from a modified U-tube tool (Fenwick, Marty & Neher, 1982). Pressure pipettes were positioned with their tips 50–400  $\mu\text{m}$  (normally about 300  $\mu\text{m}$ ) from the recording pipette. The U-tube tool, manufactured from narrow polythene tubing (0.6 or 1.1 mm external diameter) was positioned

TABLE 1. The composition of the bathing media and electrode-filling solutions. Certain other electrode-filling solutions were produced by mixing ES2 and ES3 together. All solutions were titrated to pH 7.2 with NaOH except for ES2 and ES3, where tetraethylammonium hydroxide was used. X represents isethionate

Bathing media	Concentration (mM)						
	NaCl	KCl	CaCl <sub>2</sub>	MgCl <sub>2</sub>	TEA Cl	HEPES	Glucose
BM 1	140	3.5	2	1	—	10	5
BM 2	120	3.5	2	1	20	10	5
BM 3	121	3.5	0.5	15	—	10	5
BM 4	136	3.5	0.2	6	—	10	5
Electrode-filling solutions	CsCl	NaCl	NaX	CaCl <sub>2</sub>	MgCl <sub>2</sub>	EGTA	HEPES
ES 1	140	—	—	1	2	11	10
ES 2	—	120	—	1	2	11	10
ES 3	—	6	114	1	2	11	10

about 300  $\mu\text{m}$  from the experimental preparation. The addition of phenol red to all test solutions at a final concentration of 0.66 mM enabled us to check for leakage from the U-tube. The Cs<sup>+</sup>-containing test solutions were produced by exchanging all or some of the inorganic monovalent cations in the bathing medium for Cs<sup>+</sup> on a stoichiometric basis.

To check for contamination, the bathing and test solutions were analysed using high-performance liquid chromatography (see Turnell & Cooper, 1982 for methods). No differences were detected between the amino acid profiles of the Cs<sup>+</sup>- and Na<sup>+</sup>-containing solutions used in these experiments. In both types of solution the concentration of GABA was below 70 nM, the limit of detection of the assay (defined as 3 times the peak-to-peak baseline noise). Both control and test solutions were found to contain glycine at concentrations of up to 200 nM.

The chloride activities ( $a_{\text{Cl}}$ ) of all solutions were estimated by interpolation from standard Tables (Robinson & Stokes, 1959). First the ionic strength of a given solution was calculated and then this value used to obtain the mean activity coefficient for the major salt. The mean activity coefficient was converted, if necessary, to give the activity coefficient for monovalent ions and this value used to derive the  $a_{\text{Cl}}$  of the solution.

#### Liquid junction potentials

In most experiments the recording pipette and bath contained solutions of different ionic composition and so liquid junction potentials developed between the recording pipette and the bath. All liquid junction potentials were corrected for, using a procedure identical to that described by Kaneko & Tachibana (1986). A patch pipette filled with 3 M-KCl was used as the reference electrode against which all junction potentials were measured, and was judged as an adequate reference using the method of Bjerrum (Glasstone, 1937; MacInnes, 1939). The difference between junction potentials measured using 1.5 or 3 M-KCl-filled reference electrodes was 0.2 mV and therefore the reference electrode containing 3 M-KCl was considered adequate.

## RESULTS

### *Caesium ions applied extracellularly increase the conductance of spinal cord neurones*

Fig. 1 illustrates a current-clamp recording made from a s.c. neurone using an electrode which contained 140 mM-CsCl (solution ES 1, Table 1). The cell had an initial

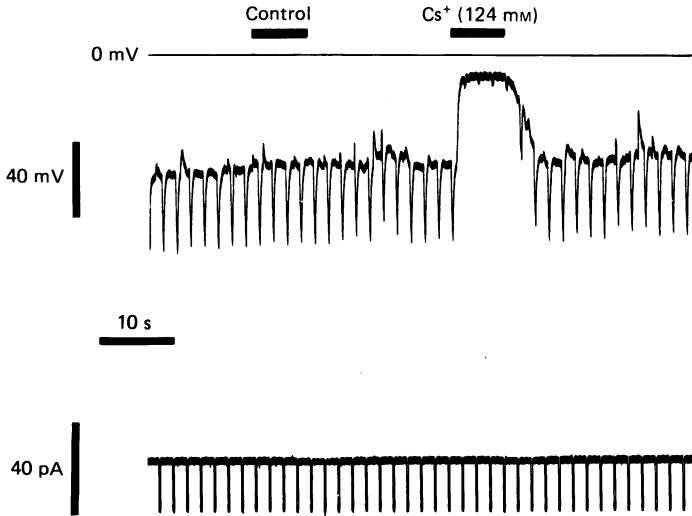


Fig. 1.  $\text{Cs}^+$  reduce the input resistance and depolarize the membrane potential of s.c. neurones. In a current-clamp recording the cell was held at around  $-60$  mV and hyperpolarizing currents injected at a frequency of  $0.55$  Hz. Control application of the bathing medium (BM2) produced no change in the membrane voltage, whereas application of the test solution (containing  $124$  mM- $\text{Cs}^+$ ) depolarized the membrane potential to  $-12$  mV and reduced the cell's input resistance (indicated by the decreased voltage response (upper trace) to the constant-current injections (lower trace)). TTX ( $0.8$   $\mu\text{M}$ ) and  $\text{CdCl}_2$  ( $100$   $\mu\text{M}$ ) were added to the test and bath (BM2) solutions. The bold horizontal bars above the voltage trace indicate the duration of control and test applications and the finer horizontal line marks  $0$  mV. The pipette-filling solution was ES1.

membrane potential of  $-73$  mV which fell slowly throughout the rest of the experiment. Application of a balanced salt solution containing  $124$  mM- $\text{Cs}^+$  to the neurone, depolarized the membrane potential and reduced the cell's input resistance (Fig. 1). Similar responses were seen in sixteen out of seventeen cells where the electrode-filling solution was solution ES1 and the bathing medium solution BM1 or BM2.

In some of these seventeen cells we altered the membrane potential by current injection, and were able to determine that the reversal potential of the  $\text{Cs}^+$ -induced response was approximately  $0$  mV. Given the ionic composition of the solutions it seemed possible that  $\text{Cs}^+$  were activating a  $\text{Cl}^-$ -specific channel.

#### *Caesium ions may induce chloride-specific currents in spinal cord neurones*

To determine the basis for the depolarization and decrease in input resistance caused by  $\text{Cs}^+$ , the  $\text{Cl}^-$  concentration of the recording pipette solution was reduced and  $\text{Cs}^+$  applied to s.c. neurones under voltage-clamp conditions.

Fig. 2A shows the result of the application of a test solution containing  $125$  mM- $\text{Cs}^+$  to an s.c. neurone containing a solution with a  $\text{Cl}^-$ -activity of  $24$  mM. The cell's membrane potential was stepped alternately between two voltages to permit its input resistance to be monitored. From the three current traces it is clear that the

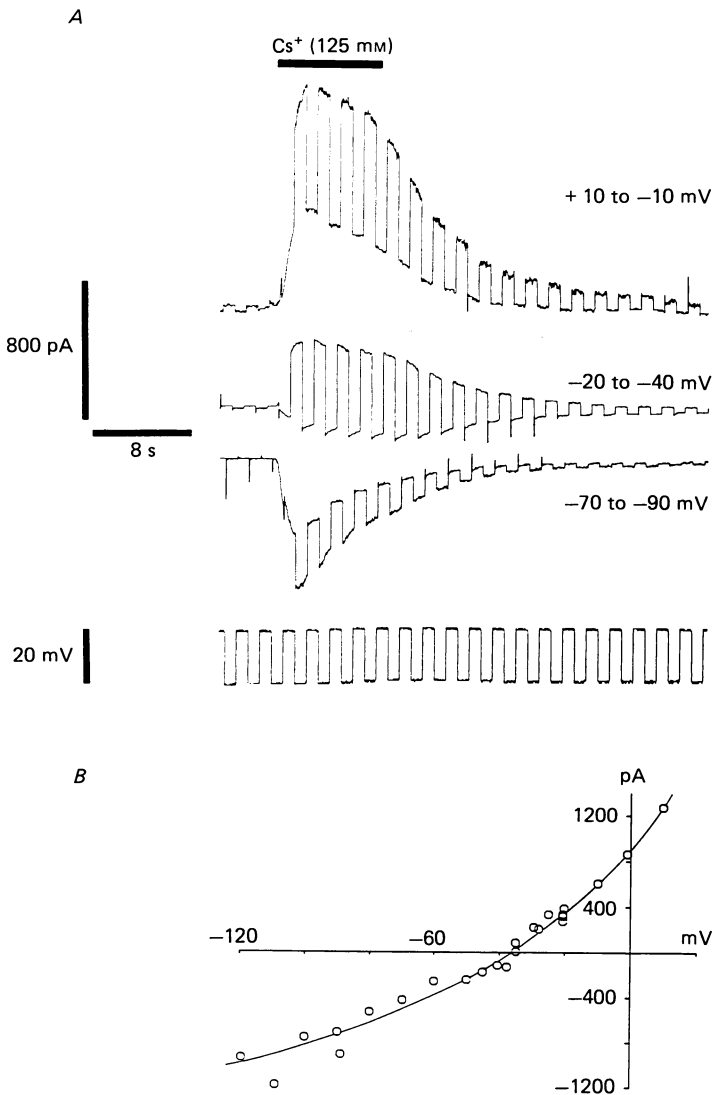


Fig. 2.  $\text{Cs}^+$  activate membrane currents that reverse near the  $\text{Cl}^-$  equilibrium potential. *A*, application of a solution containing 125 mM- $\text{Cs}^+$  to an s.c. neurone induced membrane currents and increased the conductance of the cell. The membrane voltage was stepped alternately between two values throughout the recording. An upward-going current corresponds to an outward movement of positive charge in this and all subsequent Figures. Note that the inward  $\text{Cs}^+$ -induced current at  $-40$  mV takes longer to peak than the outward current at  $-20$  mV. *B*, a graph of the maximum  $\text{Cs}^+$ -induced current *versus* the membrane voltage for this cell indicated that the reversal potential for the response was  $-36$  mV. The  $\text{Cl}^-$  equilibrium potential was  $-38$  mV. The cell was bathed in BM3 and filled with a solution consisting of (mM)  $\text{CsCl}$ , 28;  $\text{Cs}_2\text{SO}_4$ , 56;  $\text{CaCl}_2$ , 1;  $\text{MgCl}_2$ , 2; EGTA, 11; sucrose, 56; and Na HEPES, 10.

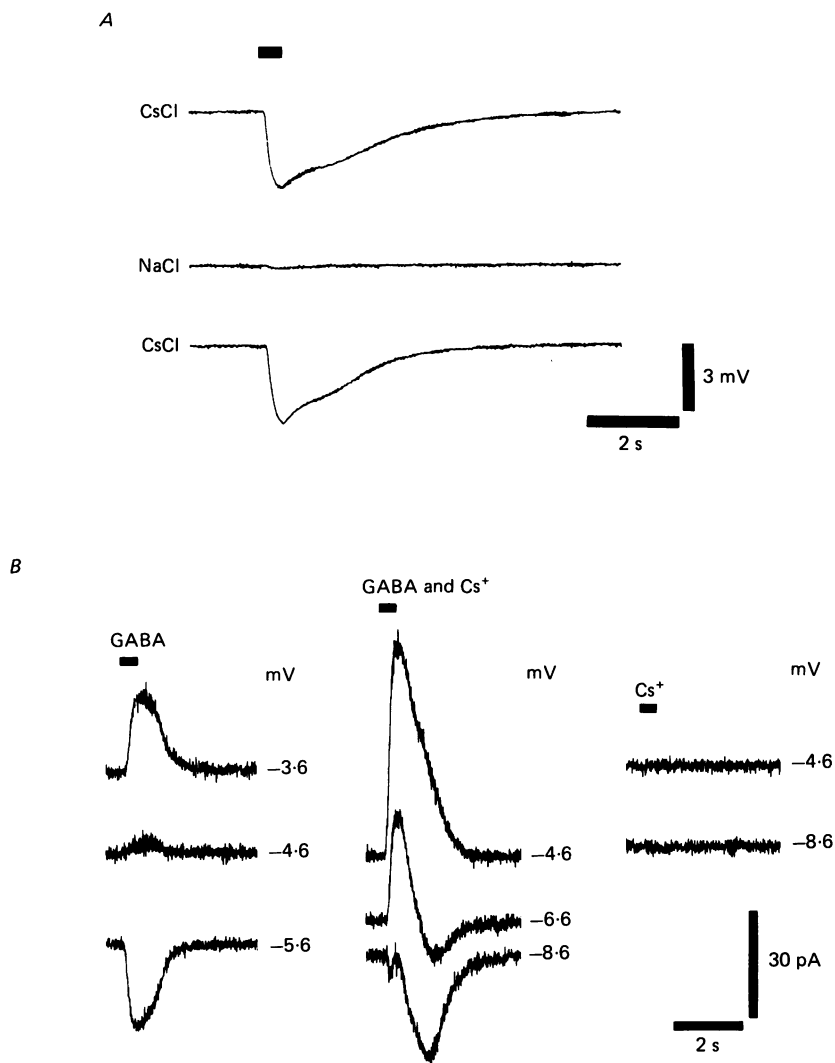


Fig. 3. Liquid junction potentials developed when the major cation in a solution was changed from  $\text{Na}^+$  to  $\text{Cs}^+$ . *A*, the liquid junction potentials that developed under zero-current conditions when solutions were applied to a patch pipette filled with a 3 M-KCl solution. The recording chamber contained solution BM1. When a solution containing 140 mM-CsCl (all  $\text{Na}^+$  exchanged for  $\text{Cs}^+$ ) was applied by U-tube tool, the potential at the patch pipette was transiently increased by  $-3.4$  mV (upper trace). A similar voltage change was seen when a solution containing  $20 \mu\text{M}$ -GABA plus 140 mM-CsCl was applied to the pipette (lower trace). No junction potential was observed when solution BM1 was applied to the pipette. *B*, the effects of 140 mM- $\text{Cs}^+$  on the GABA-activated current in pars intermedia cells. GABA ( $20 \mu\text{M}$ ) in solution BM1 induced currents that reversed at  $-4.7$  mV (left-hand trace,  $E_{\text{Cl}} = -4.3$  mV) whereas the same concentration of GABA in a solution containing 140 mM- $\text{Cs}^+$  induced currents that reversed at  $-8.4$  mV (middle trace). The application of 140 mM- $\text{Cs}^+$  did not alter the membrane current (right-hand trace). The cell was bathed in solution BM1 and solution ES2 used to fill the patch pipette. All applications were made for 0.5 s with 90 s between each application. The cell had an input resistance in solution BM1 of 15 G $\Omega$ .

Cs<sup>+</sup>-induced currents reversed somewhere between  $-20$  and  $-40$  mV and that they were associated with an increase in the cell's conductance.

A current-voltage plot of the change in membrane current induced by Cs<sup>+</sup> revealed a reversal potential of  $-36$  mV (Fig. 2*B*). The mean reversal potential of Cs<sup>+</sup>-induced currents from three such cells was  $-35 \pm 1$  mV (mean  $\pm$  s.d.) which was comparable to the Cl<sup>-</sup> equilibrium potential ( $E_{Cl}$ ) of  $-38$  mV.

Whilst this finding supported the idea that Cs<sup>+</sup> were activating a Cl<sup>-</sup> channel we observed that the inward and outward currents usually peaked at different times when the voltage steps straddled the reversal potential (see middle trace Fig. 2*A*). If we applied Cs<sup>+</sup> to s.c. neurones without using the voltage step protocol other features of the Cs<sup>+</sup>-induced currents were revealed. At voltages close to the reversal potential the currents were often biphasic, consisting of both inward and outward components, whereas further from the reversal potential they were monophasic (see Figs 4 and 5). Such differences in the currents at voltages near to the reversal potential seemed inconsistent with the hypothesis that the action of Cs<sup>+</sup> was simply to induce a Cl<sup>-</sup>-specific current. Therefore, to permit an investigation of the dependence of the Cs<sup>+</sup>-induced current on the transmembrane  $a_{Cl}$  ratio, it was first necessary to establish the basis of the biphasic currents.

#### *Two other membrane currents associated with the application of caesium ions to spinal cord neurones*

It has been reported that changing the ionic composition of the solution around a cell can lead to a membrane current as a result of the development of a liquid junction potential (Hodgkin, McNaughton & Nunn, 1985). As the ionic composition of the solution around the cell was significantly changed during the application of Cs<sup>+</sup>, we investigated whether the development of a liquid junction potential was responsible for the differences in the time courses and the biphasic nature of the currents described above.

To determine whether the application of Cs<sup>+</sup> produced a liquid junction potential, Cs<sup>+</sup>-containing solutions were applied to a 3 M-KCl-filled patch electrode that was surrounded by solution BM1. The voltage between the patch and reference electrodes was recorded under zero-current conditions. Fig. 3*A* shows that during the application of a solution containing 140 mM-CsCl the voltage around the patch electrode became more negative by 3.4 mV (upper trace). A similar change was seen when the same solution was applied with 20  $\mu$ M-GABA (lower trace); however, no measurable voltage change was associated with the application of solution BM1 (middle trace). The peak potential change produced by the application of Cs<sup>+</sup> was fairly constant ( $3.4 \pm 0.1$  mV,  $n = 12$ ) but the time course of the voltage change was more variable. The junction potential peaked within 500 ms, but the time course of decay was more sensitive to the rates at which the solutions were passed into and sucked out of the U tube.

Next, we examined the effect of the Cs<sup>+</sup>-dependent liquid junction potential on ligand-activated Cl<sup>-</sup> currents, to determine whether it could have caused biphasic currents like those observed in Figs 4 and 5. We used cells from the pars intermedia of the rat pituitary gland as they possess GABA-activated Cl<sup>-</sup> channels (Kehl & McBurney, 1986) but do not respond to Cs<sup>+</sup> (S. M. Smith & R. N. McBurney, unpublished observation). The cells were cultured according to the methods of Kehl, Hughes & McBurney (1987).

The responses shown in Fig. 3*B* are representative of the six pars intermedia cells examined. Application of GABA (20  $\mu$ M) activated monophasic currents that reversed at  $-4.7$  mV whereas the same concentration of GABA plus 140 mM-CsCl induced currents that reversed at  $-8.4$  mV. In all six cells tested the reversal potential of the GABA-induced currents was more negative in the presence of Cs<sup>+</sup>. The mean difference between the two sets of reversal potentials was  $3.0 \pm 0.6$  mV

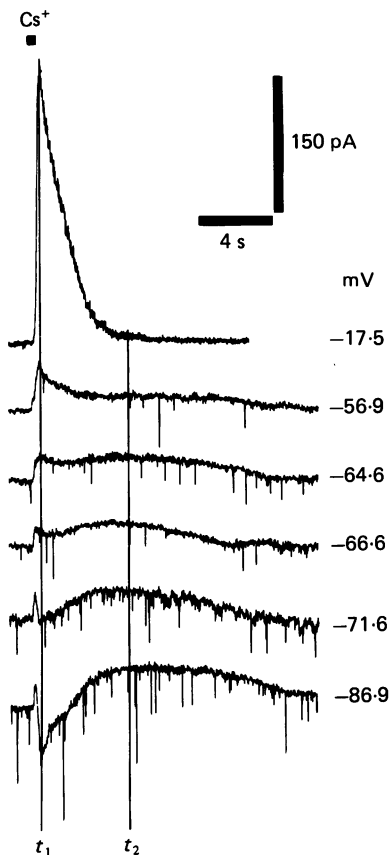


Fig. 4. The application of  $\text{Cs}^+$  (140 mM) to an s.c. neurone induced a ' $\text{Cl}^-$ ' current and a sustained outward current which was largest at negative potentials. The outward current can be seen before time  $t_1$  at  $-71.6$  and  $-86.9$  mV and clearly at time  $t_2$  at all voltages except for  $-17.5$  mV. The time taken for the current in the  $-17.5$  mV trace to peak was defined as  $t_1$ . The two vertical lines mark  $t_1$  and  $t_2$  relative to the signal from the U-tube tool that denotes the beginning of the application. The cell was bathed in a version of solution BM1 to which the 3.5 mM-KCl was not added. The patch pipette contained solution ES3. The inward transient currents were spontaneous synaptic events that reversed somewhere between 5 and  $-15$  mV. Using the method described in the text the reversal potential for the currents at  $t_1$  was measured as  $-64.7$  mV. Therefore the very small decrease in outward current between  $t_1$  and  $t_2$  observed at  $-64.6$  and  $-66.6$  mV may have been due to the liquid junction current.

and we therefore concluded that the cells were experiencing the  $\text{Cs}^+$ -induced liquid junction potential.

Fig. 3B also illustrates that at voltages near to the reversal potential  $\text{Cs}^+$  changed the monophasic GABA response to a more complicated current. As  $\text{Cs}^+$  alone had no effect on this cell (right-hand trace) we proposed that the liquid junction potential was responsible for the biphasic nature of the GABA-activated current at  $-6.6$  mV and for the increase in the time taken for the current at  $-8.6$  mV to peak. Both of these characteristics could have been produced if the GABA-activated conductance persisted longer than the  $\text{Cs}^+$ -induced change in driving voltage. It was not clear to us how such differences in the durations of the two effects might have occurred. However, in the absence of an alternative explanation we proposed that the  $\text{Cs}^+$ -induced junction potential was responsible for the modification of the GABA-induced currents illustrated in Fig. 3B.



As a consequence of the liquid junction potential the membrane voltage varied during Cs<sup>+</sup> application. We therefore measured all the currents for a given cell at the point at which outward monophasic currents peaked. This point was selected as it presumably preceded the decay of the Cs<sup>+</sup>-induced liquid junction potential.

Cs<sup>+</sup>-induced currents in s.c. neurones also showed the same behaviour as the GABA-induced currents of pars intermedia cells in the presence of Cs<sup>+</sup> (see Fig. 5A). In ten of the twenty-one s.c. neurones in which the responses were measured near the reversal potential, outward currents were biphasic and inward currents took longer to peak than the outward currents. We presumed that this was due to the Cs<sup>+</sup>-activated current being affected by the Cs<sup>+</sup>-induced junction potential and therefore we determined the reversal potentials as described above.

In two of the other eleven cells the currents appeared monophasic but in the remaining nine, in addition to the 'Cl<sup>-</sup>' current, the application of Cs<sup>+</sup> was associated with a sustained outward current (Fig. 4). These outward currents varied with the membrane voltage in two cells, increasing as the cell was hyperpolarized. In the other seven cells the outward current did not apparently vary with membrane voltage. The outward currents measured within 2 mV of the apparent reversal potential of the Cl<sup>-</sup> current varied between 7 and 100 pA (mean =  $28 \pm 29$  pA).

The nature of the sustained outward current was not investigated but certain evidence points to its resulting from the blockage of an inward Na<sup>+</sup> current by Cs<sup>+</sup>. In four cells where the input resistance and outward current were both measured, the outward current was 3.5–4.7 times greater than could be accounted for by the current flowing across the input resistance of the cell as a result of the Cs<sup>+</sup>-induced junction potential. We therefore suggest that there must be an underlying change in the cells' input resistance. The outward current was observed in the presence of intracellular Na<sup>+</sup> (nine out of sixteen cells) and the absence of extracellular and intracellular potassium ions (Fig. 4). The outward current was absent when the major intracellular cations were Cs<sup>+</sup> (five cells). In addition, the tendency of the outward current to persist beyond the application period, and only to begin to decrease between 1.5 and 5.7 s (mean =  $3.9 \pm 1.4$  s) after the application, seemed consistent with the idea that the outward current was a result of the blockage of channels (Fig. 4).

In cells in which the sustained outward current was elicited, the Cs<sup>+</sup>-induced 'Cl<sup>-</sup>' current was measured by subtracting the current at time  $t_2$  from the current at time  $t_1$  (see Fig. 4). Both currents were measured relative to the pre-application baseline. The time  $t_1$  was defined as the time at which monophasic Cs<sup>+</sup>-induced outward currents peaked and was taken to correspond to the point at which the Cs<sup>+</sup>-activated 'Cl<sup>-</sup>' conductance was at a maximum. The point  $t_2$  was defined as the time at which the Cs<sup>+</sup>-induced outward current was neither masked by the 'Cl<sup>-</sup>' current nor had begun to decrease, and was selected by inspection of the current traces at potentials within 30 mV of the reversal potential. At potentials positive to this limit it was often not possible to measure the persistent outward current because the 'Cl<sup>-</sup>' current was so much larger (see Fig. 4, -17.5 mV trace). As currents at these voltages were not used to derive the reversal potential this was not a problem in the analysis.

#### *Caesium ions induce a chloride-specific current in spinal cord neurones*

We have tentatively suggested that Cs<sup>+</sup> induce a Cl<sup>-</sup>-specific current in s.c. neurones. Having established a means of eliminating other contaminating currents,

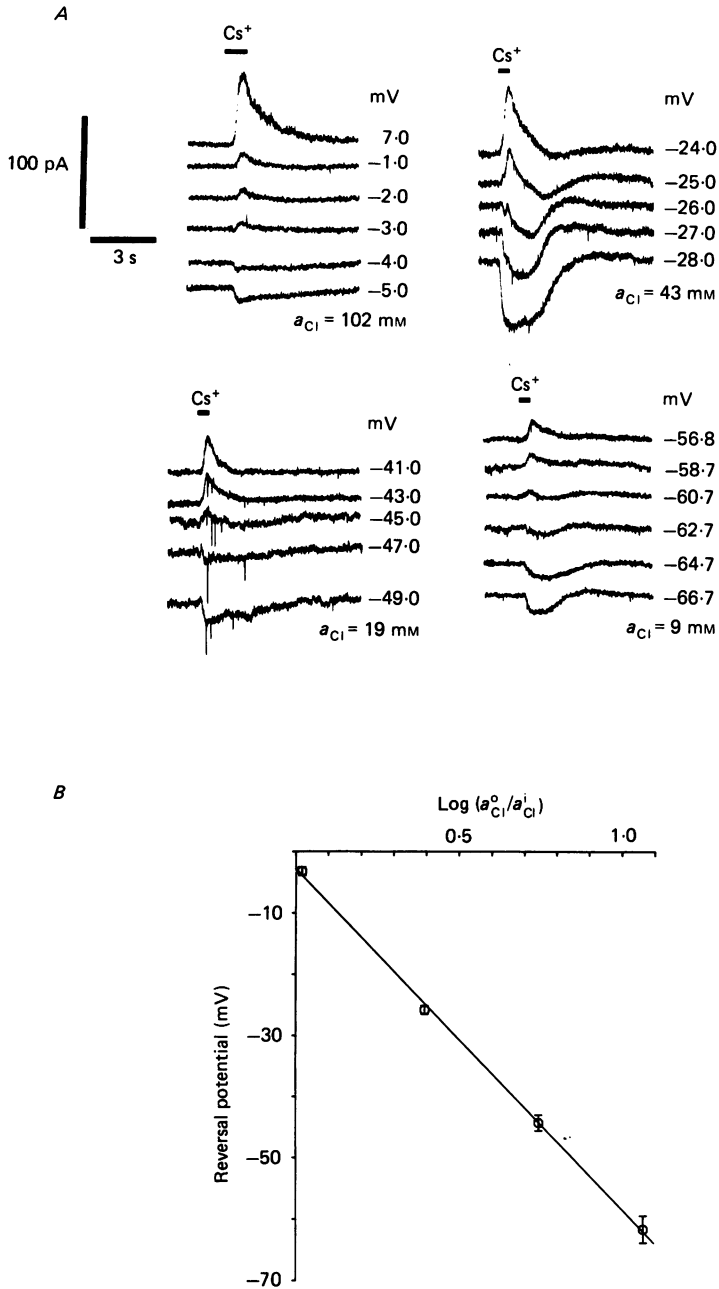


Fig. 5. The reversal potential for Cs<sup>+</sup>-induced currents follows the  $E_{Cl}$ . A, four typical sets of currents in which the ratio of the extracellular Cl<sup>-</sup> activity ( $a_{Cl}^o$ ) to the intracellular activity ( $a_{Cl}^i$ ) was different for each cell. The  $a_{Cl}^i$  values are given under each set of traces. The cell for which  $a_{Cl}^i = 9$  mm was bathed in a modified version of solution BM 1 which did not contain 3.5 mM-KCl, but the other three cells were superfused with normal solution BM 1. Solution ES 1 was used to give an  $a_{Cl}^i$  of 102 mm and all other pipette-filling solutions were made up of mixtures of solutions ES 2 and ES 3. Cs<sup>+</sup> (140 mM) were applied by U-tube for durations indicated by the horizontal bars. The reversal potentials of the

we investigated the dependence of the reversal potential of the  $\text{Cs}^+$ -induced response on the  $E_{\text{Cl}}$ . The intracellular  $a_{\text{Cl}}$  was altered by substituting isethionate ions for  $\text{Cl}^-$  on a stoichiometric basis. The size of the  $\text{Cs}^+$ -induced currents permitted us to make measurements within 1 or 2 mV of the reversal potential, as is illustrated by Fig. 5A. This minimized the amount of interpolation necessary to estimate the reversal potential. A 10-fold reduction of the intracellular  $a_{\text{Cl}}$ , for a constant extracellular  $a_{\text{Cl}}$ , shifted the reversal potential of the  $\text{Cs}^+$ -induced currents by  $-56$  mV on average (Fig. 5B). The similarity of this value to the  $-58$  mV predicted by the Nernst equation confirmed that  $\text{Cs}^+$  were activating a  $\text{Cl}^-$  current. The failure of the line in Fig. 5B to pass through the origin can be accounted for by the  $\text{Cs}^+$ -induced liquid junction potential of 3.4 mV.

#### *Caesium ions act directly on the postsynaptic cell*

Since our test solutions were not significantly contaminated by a known  $\text{Cl}^-$  channel agonist (see Methods) we considered that  $\text{Cs}^+$  might act either indirectly by releasing neurotransmitters from presynaptic terminals onto s.c. neurones, or directly at receptors in the membrane of s.c. neurones.

We applied  $\text{Cs}^+$  to s.c. neurones in the presence of high  $\text{Mg}^{2+}$  and low  $\text{Ca}^{2+}$  concentrations as these conditions were expected to block synaptic transmission (Jefferys & Haas, 1982). In seven cells that were bathed in solution BM3 or BM4, the application of a solution containing  $\text{Cs}^+$  (125 or 140 mM respectively) induced  $\text{Cl}^-$  currents (see Fig. 2A). Moreover,  $\text{Cs}^+$  activated  $\text{Cl}^-$  currents in s.c. neurones in the presence of the  $\text{Ca}^{2+}$  channel blocker,  $\text{Cd}^{2+}$  (50–100  $\mu\text{M}$ ). Both of these results support the idea that  $\text{Ca}^{2+}$ -dependent release was not involved in the  $\text{Cs}^+$ -activated response. Exclusion of this possibility led us to suggest that  $\text{Cs}^+$  were acting directly on the extracellular surface of the neuronal membrane to activate  $\text{Cl}^-$  currents.

In a later set of experiments on s.c. neurones with apparent synaptic activity,  $\text{Cs}^+$  did cause release. Such  $\text{Cs}^+$ -induced transmitter release was seen as a burst of events that were superimposed on the  $\text{Cs}^+$ -induced  $\text{Cl}^-$  current (Fig. 5A, lower left panel). Each event had a fast rising phase and an exponential decay phase (not shown).

#### *Properties of caesium-induced chloride currents*

During the prolonged application of 140 mM- $\text{Cs}^+$  to an s.c. neurone the  $\text{Cs}^+$ -activated current would typically fade (Fig. 6B). As this fading was not due to a decrease in the concentration of  $\text{Cs}^+$  being ejected from the U-tube tool (Fenwick *et al.* 1982) we tested whether it was caused by the  $\text{Cl}^-$  current altering  $E_{\text{Cl}}$  (Huguenard & Alger, 1986). First the reversal potential for the  $\text{Cs}^+$ -activated current was measured (Fig. 6A). The cell membrane potential was then held close to this value ( $-3$  mV)

---

four cells were measured by interpolation as being  $-3.5$ ,  $-26.0$ ,  $-46.2$  and  $-61.7$  mV. The inward transient currents seen for the cell where  $a_{\text{Cl}}^i$  was 19 mM were synaptic events whose frequency increased during  $\text{Cs}^+$  application. B, the plot of the reversal potential versus the logarithm of the ratio of  $a_{\text{Cl}}^o$  to  $a_{\text{Cl}}^i$  has a slope of  $-56$  mV and a correlation coefficient of 0.9996. Each point represents the mean  $\pm$  s.d. of four to six different s.c. neurones. A total of twenty-one cells were used.

but stepped to  $-63$  mV before a solution containing  $140$  mM- $\text{Cs}^+$  was applied. The  $\text{Cl}^-$  current faded during the  $3$  s period of application (Fig. 6*B*). After  $120$  s this procedure was repeated but the voltage was stepped back to  $-3$  mV after only  $2$  s of the  $\text{Cs}^+$  application period (Fig. 6*C*). There was no measurable  $\text{Cl}^-$  current at  $-3$  mV whereas the current just prior to this, at  $-63$  mV, was only  $64\%$  of its peak

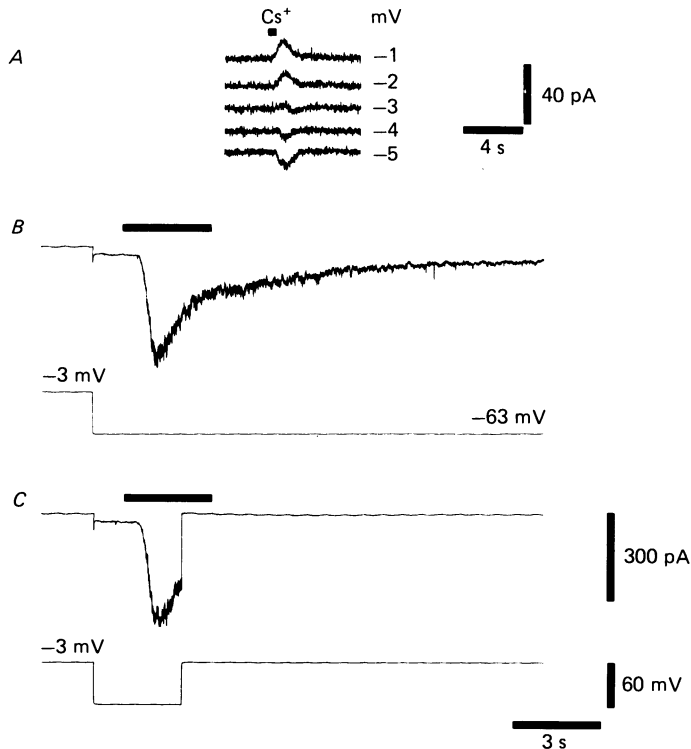


Fig. 6. A change in  $E_{\text{Cl}}$  is not responsible for the observed fading of  $\text{Cs}^+$ -induced currents during the prolonged application of  $140$  mM- $\text{Cs}^+$  (all  $\text{Na}^+$  replaced by  $\text{Cs}^+$ ). *A*, the  $\text{Cs}^+$ -induced  $\text{Cl}^-$  currents reversed polarity near to  $-3$  mV. The membrane voltage is marked next to each trace. The calibration bars are to the right of the current traces. *B*,  $\text{Cs}^+$ -induced  $\text{Cl}^-$  current at  $-63$  mV in response to the  $3$  s application of  $140$  mM- $\text{Cs}^+$ . *C*,  $\text{Cs}^+$ -induced currents at  $-63$  and  $-3$  mV in response to the application of  $140$  mM- $\text{Cs}^+$ . The calibration bars for the current and voltage traces of *B* and *C* are in the lower right-hand corner of the Figure. The bathing medium and electrode-filling solutions were BM1 and ES1 respectively. The unmarked horizontal bars denote the application of  $\text{Cs}^+$ .

value ( $340$  pA). In the absence of such a current at  $-3$  mV we concluded that the value of  $E_{\text{Cl}}$  had not changed significantly and that the fading of the  $\text{Cs}^+$ -activated response was the result of desensitization.

Caesium ions ( $140$  mM) activated  $\text{Cl}^-$  currents in the majority of s.c. neurones tested ( $94\%$ ,  $n = 69$ ). However, it was obviously essential to investigate the dose dependence of the response to  $\text{Cs}^+$  in order to assess the physiological importance of these ions. Fig. 7*A* illustrates the dependence of the size of the  $\text{Cs}^+$ -induced response on the concentration of  $\text{Cs}^+$  applied to a typical cell. The test solutions were applied

using a U-tube tool whilst the cell's voltage was held at  $-55$  mV. The dose-response curves for all six cells failed to reach a plateau with the maximum  $\text{Cs}^+$  concentration of  $140$  mM and this prevented us from obtaining the concentration of  $\text{Cs}^+$  that gave the half-maximal activation ( $K_D$ ). However, from the six dose-response curves we estimated that the  $K_D$  was on average greater than  $69$  mM.

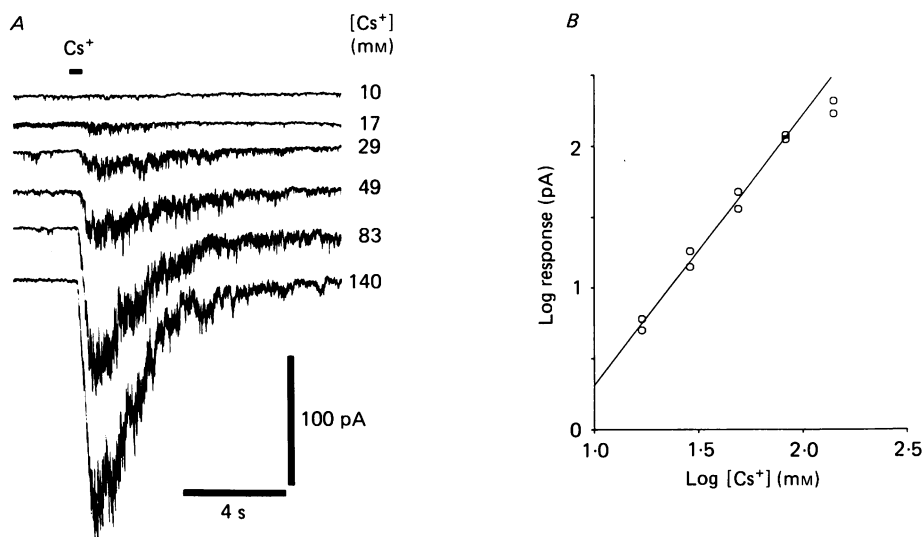


Fig. 7. The dose dependence of  $\text{Cs}^+$ -induced  $\text{Cl}^-$  currents in an s.c. neurone. *A*, the application of increasing concentrations of  $\text{Cs}^+$  (all or some of  $\text{Na}^+$  replaced by  $\text{Cs}^+$ ) induced correspondingly larger currents. All applications were made from a U-tube tool for 0.5 s with 90 s between each application while the cell was held at  $-55$  mV. In this cell only the solutions containing at least 17 mM- $\text{Cs}^+$  induced currents. *B*, the log-log plot of the maximum  $\text{Cs}^+$ -induced current *versus* the  $\text{Cs}^+$  concentration has a slope of 1.9 and a correlation coefficient of 0.995. The two values for responses to 140 mM- $\text{Cs}^+$  were not included in the linear regression as they fell below the line predicted by the other points.

The log-log plot of the maximum current *versus* the concentration of  $\text{Cs}^+$  for this cell had a gradient of 1.9 (Fig. 7*B*), and similar plots for six cells yielded a slope of  $1.7 \pm 0.4$ . However, these values may have been reduced as a result of desensitization occurring at higher concentrations of  $\text{Cs}^+$ . The slope of log-log dose-response graphs has been interpreted previously as indicating the minimum number of agonist molecules necessary to activate a channel (Sakmann, Hamill & Bormann, 1982). We therefore suggest that at least 2  $\text{Cs}^+$  bind to the receptor to activate the channel. The currents activated by 140 mM- $\text{Cs}^+$  sometimes fell below the value predicted by the other data in the log-log dose-response plot (Fig. 7*B*). It was not clear whether this was a result of the plot nearing the non-linear region prior to reaching a plateau or whether it was due to the desensitization of the receptor-channel complex.

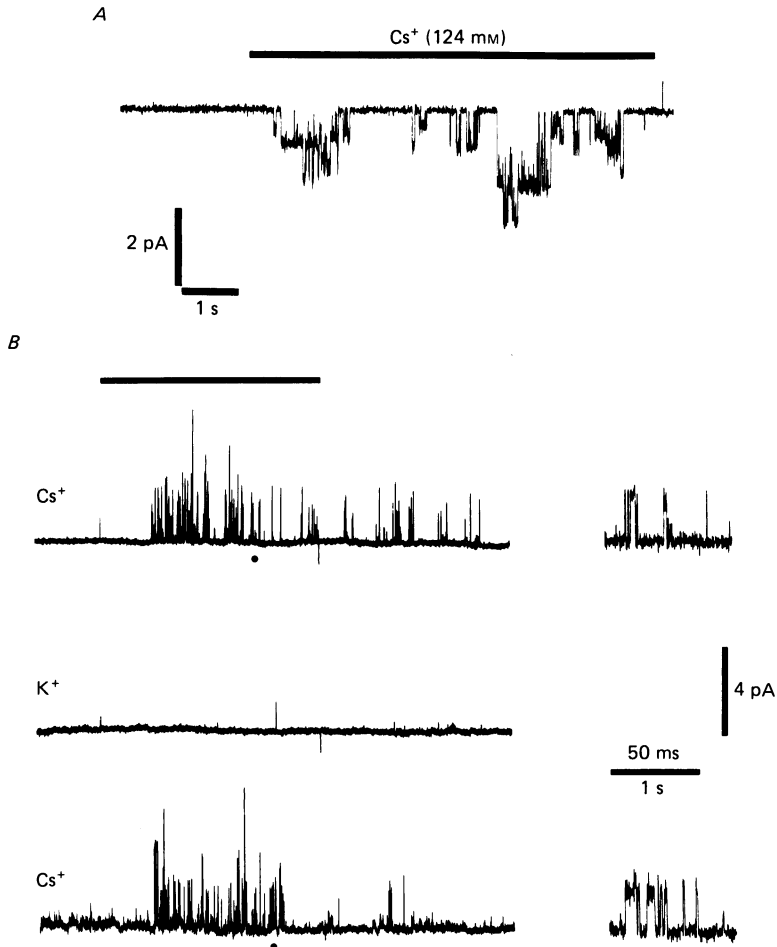


Fig. 8.  $\text{Cs}^+$  activate ion channels in membrane patches from s.c. neurones. *A*, application of a solution containing 124 mM- $\text{Cs}^+$  by pressure to an outside-out patch held at  $-25$  mV activated channels with apparently more than one conductance level. The horizontal bar marks the duration of application. TTX ( $1.6 \mu\text{M}$ ) and  $\text{Cd}^{2+}$  ( $100 \mu\text{M}$ ) were added to the bathing medium (BM2) and test solution. The patch pipette contained solution ES1. *B*, a comparison of the effects of  $\text{Cs}^+$  (140 mM) and  $\text{K}^+$  (144 mM) on an outside-out patch held at 48 mV. The 2.5 s applications (see horizontal bar) were made every 80 s from a U-tube tool. The patch pipette and recording chamber contained solutions ES1 and BM1 respectively. The insets show those parts of the current traces marked by the filled circles on an expanded time scale. Test solutions were made as for BM1 with the  $\text{Na}^+$  replaced by either  $\text{Cs}^+$  or  $\text{K}^+$ . The 50 ms calibration bar refers to the insets.

*Caesium ions activate chloride channels on the extracellular surface of patches of cell membrane*

Most outside-out patches tested were found to contain  $\text{Cs}^+$ -activated channels (86% ;  $n = 118$ ) when  $\text{Cs}^+$  were applied to their extracellular surface at concentrations of 7–144 mM. The single-channel currents were time-locked to each application and

usually displayed more than one level (Fig. 8A). Although this action of  $\text{Cs}^+$  was not shared by  $\text{Na}^+$  (Fig. 1) we tested whether  $\text{K}^+$  would activate  $\text{Cl}^-$  channels in the membranes of s.c. neurones as they are also alkali metal ions. In eleven outside-out patches  $\text{Cs}^+$  (140 mM) activated  $\text{Cl}^-$  channels, whereas a solution containing 144 mM- $\text{K}^+$  did not (see Fig. 8B). Patches with demonstrable  $\text{K}^+$  channel activity were not included in this study as such activity would have prevented an unequivocal comparison of the relative effects of  $\text{Cs}^+$  and  $\text{K}^+$ . The inability of  $\text{Na}^+$  and  $\text{K}^+$  to activate the  $\text{Cl}^-$  current suggested that  $\text{Cs}^+$  were acting at sites that possessed a degree of specificity.

Further support for the idea that  $\text{Cs}^+$  operate at specific sites came from the finding that  $\text{Cs}^+$  only acted at the extracellular surface of the neuronal membrane. We applied  $\text{Cs}^+$  (140 mM) to the intracellular surface of nine inside-out patches which were bathed on both sides with solution BM 1. Single-channel currents were not seen in any of these patches in response to  $\text{Cs}^+$  application. The application of a  $\text{K}^+$ -rich solution (as used in Fig. 8B) demonstrated the existence of  $\text{K}^+$  channels in these patches and confirmed that the patches had not formed vesicles. A  $\chi^2$  test revealed that the probability of all nine inside-out patches not containing  $\text{Cs}^+$ -activated channels was less than 0.001, assuming an identical probability of occurrence of  $\text{Cs}^+$ -activated channels in inside-out and outside-out patches. We therefore concluded that  $\text{Cs}^+$  only activated  $\text{Cl}^-$  channels by acting at the extracellular surface of the cell membrane.

#### *Conductance states of caesium-activated chloride channels*

By measuring the current amplitudes of a number of channel openings in an outside-out patch at a fixed holding potential and examining the distribution of the amplitudes, we demonstrated that the  $\text{Cs}^+$ -activated channels existed in a finite number of discrete conductance states (Fig. 9A and B). Fig. 9B illustrates one patch where most channel openings fell into one of three current levels, although a few openings to larger or smaller levels were seen. Measurement of the current levels at other voltages revealed that a total of four conductance states were exhibited by the  $\text{Cs}^+$ -activated channels in this patch and that under conditions where pipette and bathing solutions (ES 1 and BM 1) had similar  $a_{\text{Cl}}$  values (102 and 107 mM respectively) the current-voltage relationship was linear (Fig. 9C). The slopes of the lines fitted to the current-voltage data gave mean conductances of 21, 29, 45 and 65 pS for the four states.

Examination of the current-voltage data from the twenty-two patches studied using solutions with the same  $a_{\text{Cl}}$  values as above, revealed that the conductance values fell into five groups. Therefore, by pooling all the current-voltage data within each group we were able to obtain a mean value for each conductance state. The mean conductances obtained were 20, 30, 43, 66 and 92 pS (Fig. 10). On four occasions openings to states with lower conductances were seen but were not included here as their extrapolated reversal potential was  $-21$  mV.

Usually, following the brief opening of a  $\text{Cs}^+$ -activated channel, closure to a non-conducting state was seen (see Fig. 8A). However, occasionally partial closures to another discrete conductance state occurred. Following these partial closures the channel either returned to the original conductance state or closed fully (Fig. 11A).

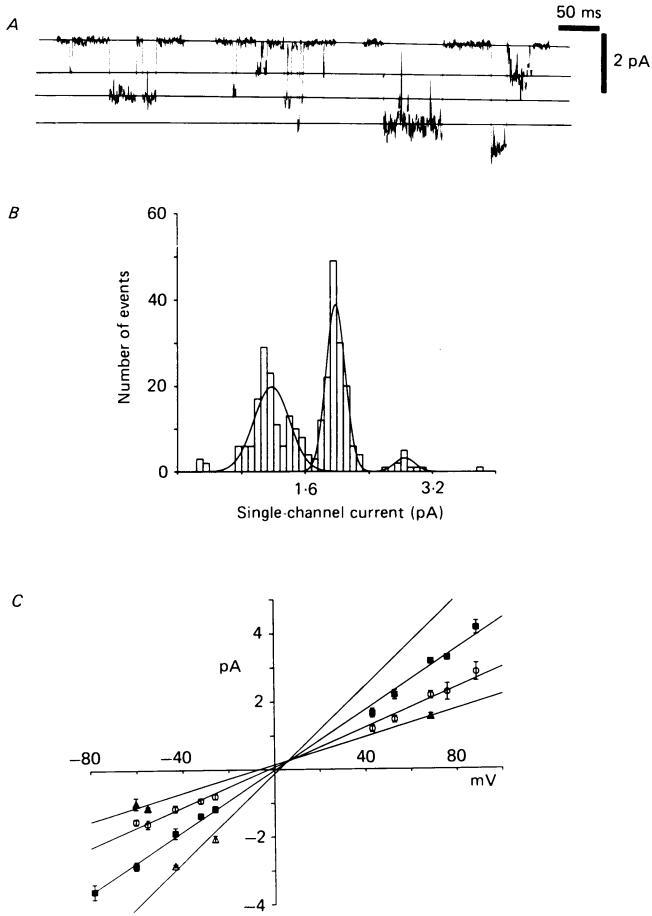


Fig. 9. Cs<sup>+</sup>-activated channels exist in a number of discrete conductance states. *A*, three current traces from an outside-out patch, held at -45 mV, with at least three Cs<sup>+</sup>-activated single-channel current levels. The four horizontal lines represent the baseline and the three mean current amplitudes obtained from the histogram. Cs<sup>+</sup> (144 mM) were added by pressure application. *B*, the histogram of the number of occurrences of the different current levels at -44 mV. The three gaussian curves have means  $\pm$  s.d. of  $1.16 \pm 0.21$ ,  $1.92 \pm 0.11$  and  $2.74 \pm 0.12$  pA. *C*, the current-voltage characteristics of the four conductance states reveal conductances of 21, 29, 45 and 65 pS. The electrode-filling solution and bathing medium were ES1 and BM1 respectively.

The frequency of movement between different conductance states was low overall but much higher at certain times. Such behaviour indicated that the phenomenon was not the result of a closing of one channel and the simultaneous opening of another channel to a different conductance state. We have therefore concluded that at least some of the Cs<sup>+</sup>-activated channels can exist in more than one conductance state.

In agreement with the data for whole-cell recordings the reversal potential for Cs<sup>+</sup>-activated single-channel currents in patches was dependent on the  $a_{Cl}$  on either side of the membrane (Fig. 11 *B*). The current-voltage plots for the three conductance states observed in the outside-out patch illustrated in Fig. 11 *B* were recorded with



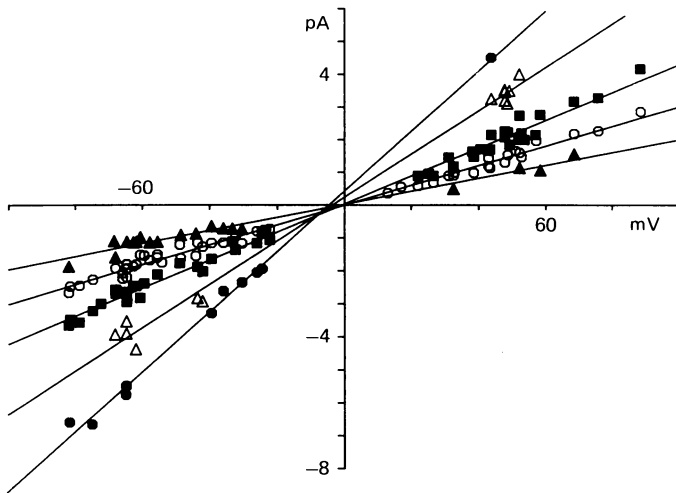


Fig. 10. The composite current-voltage plot for five distinct  $\text{Cs}^+$ -activated conductance states. The slopes of the lines give mean conductances of 20, 30, 43, 66 and 92 pS, with correlation coefficients of 0.988, 0.996, 0.996, 0.997 and 0.998 respectively. The pipette solution and bathing media were ES 1 and BM 1 or BM 2 respectively with  $a_{\text{Cl}}$  values of 102 and 112 mM respectively. The  $a_{\text{Cl}}$  value for the test solution which contained 124 or 144 mM-CsCl was 107 mM. The permeability coefficients of the five conductance states were calculated from the Goldman-Hodgkin-Katz equation as 5.0, 7.5, 10.7, 16.4 and  $22.9 \times 10^{-14} \text{ cm}^3 \text{ s}^{-1}$  assuming an equal  $a_{\text{Cl}}$  on either side of the membrane of 105 mM and a temperature of 20 °C.

$a_{\text{Cl}}$  values of 25 and 107 mM in the pipette and bath solutions respectively. The curves are Goldman-Hodgkin-Katz plots drawn using permeability coefficients of  $10.7$ ,  $7.5$  and  $3.5 \times 10^{-14} \text{ cm}^3 \text{ s}^{-1}$ .

*An attempt to describe the frequency of occurrence of the different caesium-activated conductance states*

Application of  $\text{Cs}^+$  to outside-out patches often resulted in the overlapping activation of a large number of channels. In such cases it was not possible to identify which conductance state was activated, and this prevented us from measuring the relative probability of occurrence of each conductance state precisely. However, by examining those parts of a current trace where it was possible to resolve single-channel openings from the current baseline, we obtained a crude measure of the relative frequency of different conductance states. The current trace was inspected and the most frequent current amplitude noted. The conductance state of the most frequent current amplitude was then identified from the current-voltage graphs. These measurements enabled us to estimate the probability with which a given state was the most frequently occurring state during a given application of  $\text{Cs}^+$  and the probability that a state was activated (excluding subconductance states) at least twice during any application (Table 2).

From our analysis of twenty-two outside-out patches it can be seen that the 30 and 43 pS states were observed in 73 and 72% respectively of the seventy-one different

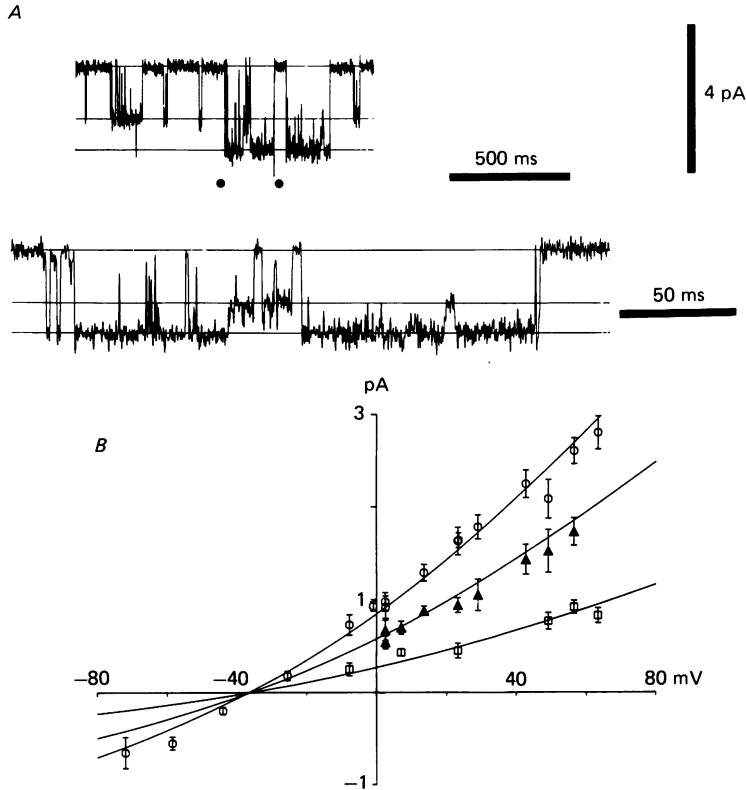


Fig. 11. A given  $\text{Cs}^+$ -activated channel can exist in more than one of the  $\text{Cl}^-$ -specific conductance states. *A*, a  $\text{Cs}^+$ -activated channel exhibits two different conductance states in an outside-out patch held at  $-20$  mV. In the upper trace discrete openings to two distinct current levels were observed. An expansion of the upper trace between the two filled circles revealed that the channel occasionally closed partially to the lower of the two states. The three continuous lines mark the current baseline and two current levels. The pipette solution was similar to ES1 except tris(hydroxymethyl)aminomethane hydrochloride was used instead of CsCl. A solution containing (mM) CsCl, 30;  $\text{Cs}_2\text{SO}_4$ , 55;  $\text{MgCl}_2$ , 1;  $\text{CaCl}_2$ , 2; sucrose, 70; Na HEPES, 10 was applied directly to the bath. *B*, the current-voltage plot of three distinct  $\text{Cs}^+$ -activated conductance states from another outside-out patch. The error bars represent standard deviations. The test solution, which contained 124 mM- $\text{Cs}^+$  and was based on BM2, was administered by bath application. The pipette solution was identical to the bath solution described in *A*. The continuous curves are Goldman-Hodgkin-Katz plots made with permeability coefficients of 10.7, 7.5 and  $3.5 \times 10^{-14} \text{ cm}^3 \text{ s}^{-1}$  using  $a_{\text{Cl}}$  values of 25 and 107 mM for the pipette and bath solutions respectively and a temperature of  $20^\circ \text{C}$ .

applications of  $\text{Cs}^+$  (Table 2). The 20, 66 and 92 pS states were observed at a fewer number of voltages. In addition, the 30 and 43 pS states were clearly seen to occur most frequently on a greater number of occasions than the other states. Taken together, these two crude measures indicate that the  $\text{Cs}^+$ -activated channel usually opens to either the 30 or 43 pS state.

TABLE 2. Column A: probability that a given conductance state was the most frequent state during any application of Cs<sup>+</sup>. Column B: probability that a state was activated at least twice during any application of Cs<sup>+</sup>. In fifteen of the applications of Cs<sup>+</sup> to outside-out patches it was not possible to identify one state as the most frequent. For this reason the sum of probabilities in column A was less than 1

Conductance state (pS)	A	B
20	0.01	0.27
30	0.38	0.73
43	0.35	0.72
66	0.04	0.30
92	0	0.14
Number of patches	22	22
Number of applications	71	71

## DISCUSSION

As the opening of Cl<sup>-</sup> channels following the application of Cs<sup>+</sup> to s.c. neurones was neither a result of contamination of our test solutions, nor due to Cs<sup>+</sup> evoking the release of a neurotransmitter from presynaptic terminals, we have concluded that Cs<sup>+</sup> act at a specific membrane site or receptor to produce this effect. Other indirect evidence consistent with the idea that Cs<sup>+</sup> act at a receptor has come from our demonstration that the Cs<sup>+</sup>-activated response desensitizes with high concentrations of agonist. This is consistent with the behaviour of many other ligand-activated channels in the presence of high concentrations of the ligand (Katz & Thesleff, 1957; McBurney & Barker, 1978).

The finding that Cs<sup>+</sup> but not Na<sup>+</sup> or K<sup>+</sup> ions activate Cl<sup>-</sup> channels, indicates that the receptor exhibits a certain specificity. However, given the concentration of Cs<sup>+</sup> needed to activate these channels ( $K_D > 69$  mM), the same finding also leads one to conclude that these Cl<sup>-</sup> channels will not be activated by alkali metal ions under normal physiological conditions. This contrasts with the alkali metal ion-activated Cl<sup>-</sup> channel which has been identified in molluscan neurones (Kislov & Kazachenko, 1975; Geletyuk & Kazachenko, 1985).

In the light of the failure of Na<sup>+</sup> and K<sup>+</sup> to activate this channel, the question arises as to what, if any, is the normal physiological function of the Cs<sup>+</sup>-activated channel in s.c. neurones? We are as yet unable to answer this question, but one possible explanation is that Cs<sup>+</sup> may be activating Cl<sup>-</sup> channels that are more normally activated by GABA and glycine in this preparation (McBurney, Smith & Zorec, 1985a). A comparison of the conductance states of the Cs<sup>+</sup>-activated channel with those obtained for GABA- and glycine-activated channels gives some substance to this hypothesis. The values of the three lowest-conductance open states of the Cs<sup>+</sup>-activated channel (20, 30 and 43 pS) are very similar to values that have been obtained for GABA- and glycine-activated states (19 and 30 pS and 21, 31 and 45 pS respectively: Hamill, Bormann & Sakmann, 1983; 20, 30 and 44 pS and 21, 32 and 46 pS respectively: McBurney *et al.* 1985a). This striking similarity in the conductances of three of the states has us to propose that Cs<sup>+</sup> activate the same type of channel as both GABA and glycine. We believe that the 66 and 92 pS states may correspond to the higher conductance levels that have been observed occasionally for

GABA- and glycine-activated channels (Hamill *et al.* 1983; R. N. McBurney, S. M. Smith & R. Zorec, unpublished observations).

Further experiments are needed to determine whether Cs<sup>+</sup> are acting directly at the GABA or glycine receptors, or whether they act at another receptor site that is also coupled to the same type of Cl<sup>-</sup> channel as the GABA and glycine receptors. However, the observation that Cs<sup>+</sup> do not activate the GABA-receptor-coupled Cl<sup>-</sup> channel in pars intermedia cells indicates that Cs<sup>+</sup> do not act via all GABA receptors.

In conclusion, we have shown that in addition to their well-known K<sup>+</sup> channel blocking properties, Cs<sup>+</sup> can activate Cl<sup>-</sup> channels which have the same conductance properties as those activated by GABA and glycine.

We thank Dr D. S. Parker for help with the high-performance liquid chromatography and Dr S. J. Kehl for preparing the pars intermedia cultures. We are grateful to Professor M. Kordas for helpful comments on the manuscript and to Professor D. D. Dolar and Dr R. D. Armstrong for helpful discussion. S.M.S. holds a Hunter Memorial Studentship. R.Z. was supported by the British Council, the Wellcome Trust and the Research Community of Slovenia.

#### REFERENCES

- COREY, D. P. & STEVENS, C. F. (1983). Science and technology of patch-recording electrodes. In *Single-Channel Recording*, ed. SAKMANN, B. & NEHER, E., pp. 53–68. New York: Plenum.
- FENWICK, E. M., MARTY, A. & NEHER, E. (1982). A patch clamp study of bovine chromaffin cells and of their sensitivity to acetylcholine. *Journal of Physiology* **331**, 577–597.
- GELETYUK, V. I. & KAZACHENKO, V. N. (1985). Single Cl channels in molluscan neurones: multiplicity of the conductance states. *Journal of Membrane Biology* **86**, 9–15.
- GLASSTONE, S. (1937). *The Electrochemistry of Solutions*. Methuen.
- HAMILL, O. P., BORMANN, J. & SAKMANN, B. (1983). Activation of multiple conductance state chloride channels in spinal neurones by glycine and GABA. *Nature* **305**, 805–808.
- HAMILL, O. P., MARTY, A., NEHER, E., SAKMANN, B. & SIGWORTH, F. J. (1981). Improved patch clamp techniques for high resolution current recording from cells and cell free membrane patches. *Pflügers Archiv* **391**, 85–100.
- HILLE, B. (1984). *Ionic Channels of Excitable Membranes*. Sunderland, MA, U.S.A.: Sinauer.
- HODGKIN, A. L., MCNAUGHTON, P. A. & NUNN, B. J. (1985). The ionic selectivity and calcium dependence of the light-sensitive pathway in toad rods. *Journal of Physiology* **358**, 447–468.
- HUGUENARD, J. R. & ALGER, B. E. (1986). Whole-cell voltage-clamp study of the fading of GABA-activated currents in acutely dissociated hippocampal neurones. *Journal of Neurophysiology* **56**, 1–18.
- JEFFERYS, J. G. R. & HAAS, H. L. (1982). Synchronised bursting of CA1 hippocampal pyramidal cells in the absence of synaptic transmission. *Nature* **300**, 448–450.
- KANEKO, A. & TACHIBANA, M. (1986). Effects of  $\gamma$ -aminobutyric acid on isolated cone photoreceptors of the turtle retina. *Journal of Physiology* **373**, 443–461.
- KATZ, B. & THESLEFF, S. (1957). A study of the desensitization produced by acetylcholine at the motor end plate. *Journal of Physiology* **138**, 63–80.
- KEHL, S. J., HUGHES, D. & MCBURNEY, R. N. (1987). A patch-clamp study of  $\gamma$ -aminobutyric acid-induced whole-cell currents in isolated pars intermedia cells of the rat. *British Journal of Pharmacology* (in the Press).
- KEHL, S. J. & MCBURNEY, R. N. (1986). Analysis of membrane currents induced by  $\gamma$ -aminobutyric acid in isolated cells of the rat pars intermedia. *Proceedings of the International Union of Physiological Societies* **16**, 551.
- KISLOV, A. N. & KAZACHENKO, V. N. (1975). Potassium activation of chloride conductance in isolated snail neurones. *Studia biophysica* **48**, 151–153.
- MCBURNEY, R. N. & BARKER, J. L. (1978). GABA-induced conductance fluctuations in cultured spinal cord neurones. *Nature* **274**, 596–597.
- MCBURNEY, R. N. & NEERING, I. R. (1985). The measurement of changes in intracellular free

- calcium during action potentials in mammalian neurones. *Journal of Neuroscience Methods* **13**, 65-76.
- MCBURNEY, R. N., SMITH, S. M. & ZOREC, R. (1985*a*). Conductance states of  $\gamma$ -aminobutyric acid and glycine activated chloride channels in rat spinal neurones in cell culture. *Journal of Physiology* **365**, 87*P*.
- MCBURNEY, R. N., SMITH, S. M. & ZOREC, R. (1985*b*). Extracellular caesium ions activate a chloride permeability in rat cultured spinal cord neurones. *Journal of Physiology* **367**, 68*P*.
- MACINNES, D. A. (1939). *The Principles of Electrochemistry*. New York: Reinhold.
- ROBINSON, R. A. & STOKES, R. H. (1959). *Electrolyte Solutions*. London: Butterworths.
- SAKMANN, B., HAMILL, O. P. & BORMANN, J. (1982). Activation of chloride channels by putative inhibitory transmitters in spinal cord neurones. *Pflügers Archiv* **392**, R19.
- TURNELL, D. C. & COOPER, J. D. H. (1982). Rapid assay for amino acids in serum or urine by precolumn derivatisation and reversed phase liquid chromatography. *Clinical Chemistry* **28**, 527-531.